The Arcus soft x-ray grating spectrometer explorer

Smith, Randall

Randall K. Smith, "The Arcus soft x-ray grating spectrometer explorer," Proc. SPIE 11444, Space Telescopes and Instrumentation 2020: Ultraviolet to Gamma Ray, 114442C (22 December 2020); doi: 10.1117/12.2576047

SPIE.

Event: SPIE Astronomical Telescopes + Instrumentation, 2020, Online Only

The Arcus Soft X-ray Grating Spectrometer Explorer

Randall Smith*[a] for the Arcus Team
[a]Center for Astrophysics | Harvard & Smithsonian, 60 Garden St., Cambridge, MA 02138

ABSTRACT

Arcus will provide high-resolution soft X-ray spectroscopy in the 12-50Å bandpass with sensitivity orders of magnitude higher than any previous astronomical observatory. The three top science goals for *Arcus* are to (1) measure the effects of structure formation imprinted upon the hot baryons that are predicted to lie in extended halos around galaxies, groups, and clusters, (2) trace the propagation of outflowing mass, energy, and momentum from the vicinity of the black hole to extragalactic scales as a measure of their feedback and (3) explore how stars form and evolve. *Arcus* uses 12m focal length grazing-incidence silicon pore X-ray optics (SPO) identical to those developed for the *Athena* mission, including focal length and radius of curvature. The focused X-rays from these optics are diffracted by high-efficiency Critical-Angle Transmission (CAT) gratings, and the results are imaged with flight-proven CCD detectors and electronics.

Keywords: X-ray gratings, X-rays: Spectroscopy, Missing baryons, Explorer missions

1. INTRODUCTION

The evolution of the structure of the Universe persists as one of the central but elusive mysteries of modern astrophysics. This structure was initially created via the gravitational collapse of non-baryonic 'Dark Matter,' which in turn shaped the distribution of 'normal' baryonic matter. The processes of collapse and subsequent evolution heated and shocked the majority of baryons, exposing them to the dramatic effects of feedback from black holes and star formation. This creates an ambient medium of tenuous, hot, metal-enriched gas that contains most of the baryonic matter and is the ultimate reservoir of entropy, metals, and the imprint of cosmic feedback. This critical component of baryonic matter has been difficult to characterize due to the low sensitivity and limited resolution of existing instruments, particularly in the X-ray regime. As a result, theory has raced ahead of observation. The EAGLE simulation shown in Figure 1 illustrates one possible distribution of hot gas as traced by O VII. The gas is concentrated around galaxies, groups, and larger structures but in these simulations extends far past the virial radius – roughly speaking, the distance where gravitational attraction no longer dominates – of these structures. These hot baryons, both in the interstellar and intergalactic media, determine the properties of the galaxies we see today.

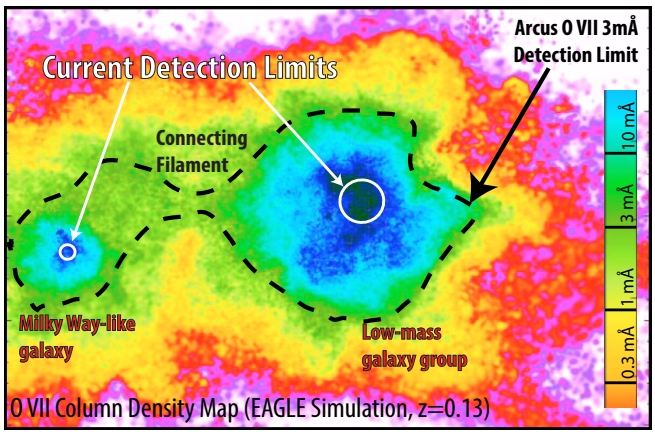

Figure 1: EAGLE simulation [4] of hot gas (seen in O VII) surrounding a low-mass galaxy group and a Milky Way-like galaxy [5]. *Arcus* will measure gas properties in the filaments connecting the two widely separated (~1.5 Mpc) systems

In pursuit of this knowledge we propose *Arcus*: the most sensitive X-ray spectrometer ever flown. In 2017 *Arcus* was selected by NASA for a MIDEX Phase A study and ultimately found to have outstanding science merit and implementation, but not selected as the *SPHEREx* mission had overall lower risk. We describe here an improved mission, modified to take advantage of technology improvements that significantly reduce risk. *Arcus* has been designed to achieve three primary goals, all top-level priorities of the 2010 Decadal Survey [1], the 2013 NASA Roadmap [2] and the 2014 NASA Strategic Plan [3]. As these priorities were also part of the 2000 and 1990 Decadal surveys, and require a sensitive X-ray spectrometer to complete, we expect them to be vital to the 2020 Decadal as well. The first goal is to determine how baryons cycle in and out of galaxies. This requires measurement of the distribution and temperature of the dominant hot gas around galaxies and clusters and maps of the temperature and abundances of gas in and around our own Galaxy. Second, understanding how feedback from a black hole system influences its surroundings. This requires determining the mass, energy and momentum in the accretion-driven, outflowing winds from both supermassive and stellar mass black holes. Third, examining how stellar systems form and evolve. This requires measuring the balance between accretion and outflow and its impact on structure formation on

Space Telescopes and Instrumentation 2020: Ultraviolet to Gamma Ray, edited by Jan-Willem A. den Herder
Shouleh Nikzad, Kazuhiro Nakazawa, Proc. of SPIE Vol. 11444, 114442C · © 2020 SPIE
CCC code: 0277-786X/20/$21 · doi: 10.1117/12.2576047

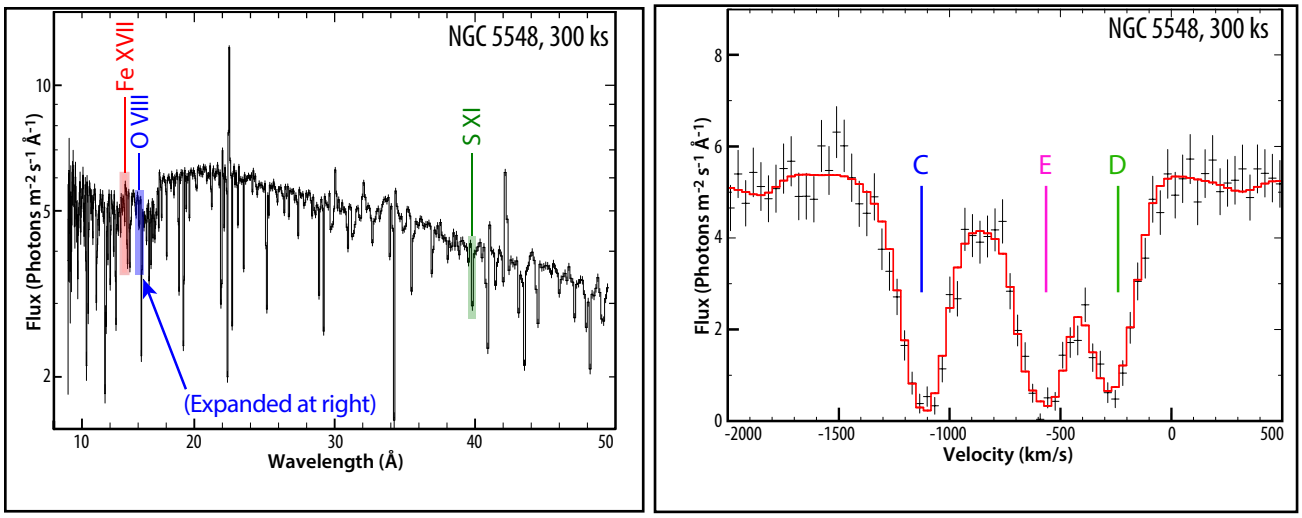

Figure 2: [Left] *Arcus* will allow the disentangling of multiple absorption components in an AGN spectrum. This simulated 300-ks spectrum of NGC 5548 has six absorption components with distinct ionization parameters and outflow velocities. The blue, green and red boxes indicate the regions of O VIII, S XI and Fe XVII, respectively. [Right] *Arcus* will fully resolve the O VIII absorption features in AGN, as indicated in this detail of the O VIII Lyβ line from the simulated NGC 5548 spectrum. Three of the six absorption components contribute to this line (components C, D and E); the other components have too low or too high an ionization parameter to produce O VIII.

the smallest scales by surveying young accreting stars, evolved coronal stars and exoplanet atmospheres.

The *Arcus* mission accomplishes these goals at low cost and risk using demonstrated technologies. *Arcus* also complements other high-profile ground and space missions that will be operating in the next decade to probe the large-scale structure of the Universe, including *LSST, Euclid, Roman Space Telescope, ALMA, JWST* and *E-ELT/GMT/TMT*.

2. SCIENCE

The Decadal Survey, NASA Roadmap, and Astrophysics Science Plan [1,2,3] all identify high-resolution X-ray spectroscopy as key to answering major open questions in astrophysics. Recent microwave [23] and X-ray observations [24] support the gravitational-collapse structure formation scenario but cannot detect individual structures. No current or planned mission offers the instrumentation necessary to provide direct observational evidence for this 'hot' component of normal matter in the Universe. While the forthcoming *XRISM* [6] and *Athena* [7] microcalorimeters promise high-resolution X-ray spectroscopy above 2 keV, finding and characterizing the "missing baryons" requires an X-ray grating spectrometer with an order-of-magnitude advance in spectral sensitivity and resolution in the 12-50 Å (0.25-1 keV) range where the key diagnostic lines lie.

The *Arcus* science objectives rely upon detecting and characterizing these critically important strong and weak lines. For a strong line, the signal-to-noise (S/N) is proportional to the square root of the product of the area and observing time. For a weak line, such as the faint absorption features expected from the intergalactic medium, the S/N is proportional to the square root of the product of the area, time, and spectral resolution. The team has performed detailed simulations that show the baseline observing plan, which consists of sources of known fluxes, can be executed with substantial margin in a 2-year baseline mission in which *Arcus*:

Assays the hot gas at and beyond the edge of galaxies and clusters, as well as the gas and dust within the Galaxy. Hot halos of gas surrounding galaxies and clusters will be studied in detail by measuring their X-ray absorption properties using the continua of bright background sources. Measuring the spatial and temperature distribution of this absorbing gas, with special attention to the gas in the Milky Way, provides the first complete picture of the formation and cycling of metals in and out of galaxies and clusters.

Determines the mass, energy and composition of outflowing winds from the inner regions of supermassive and stellar mass black holes. Actively-feeding black holes produce X-ray continuum emission that is absorbed by the outflowing hot gas. Characterizing this absorption reveals the velocity, density, and total momentum carried away by such outflows, as shown in the simulation of NGC 5548 in Figure 2. Measuring these properties with velocity resolutions comparable to other bandpasses, will reveal how black holes power winds and how the winds interact with cooler gas in the surrounding galaxy, seeding this gas with energy and ultimately regulating star formation.

Measures the thermodynamic properties of hot gas in stellar magnetic structures and shocks. Coronal X-ray emission reveals the actions of internal magnetic dynamos. Measuring X-ray fluxes from a statistical sample of stars yields both coronal temperatures and dependencies on stellar rotation and age. *Arcus* also probes the final stages of star formation in which accreting material from the protoplanetary disk creates a shock front near the stellar surface. Modeling the resulting X-ray emission provides insights into how the accretion streams interact with stellar magnetic fields.

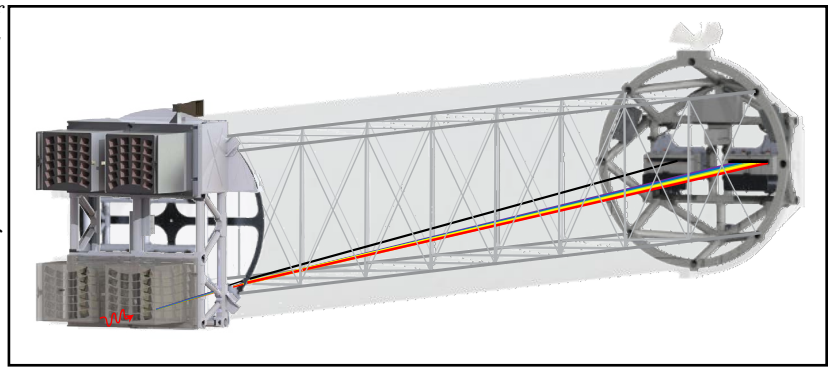

Figure 3: Schematic of the *Arcus* spectrometer, showing X-rays entering the Foward Assembly (FA) containing the optics and gratings petal and the diffracted light traveling to the CCDs mounted on the Rear Assembly (RA) to be read out by the Instrument Control Unit. The two assemblies are separated by a 10.8m long boom that supports the 12m focal length and is covered by a Germanium Black Kapton© sock (not shown).

3. INSTRUMENTATION

The keys to a successful X-ray spectroscopy mission are spectral resolution and area combined with efficient observing and low background. *Arcus*' design philosophy addresses the first two using demonstrated modular optics and gratings technologies and the latter two with a well-planned mission design. The *Arcus* spectrometer (Figure 3) focuses X-rays using Silicon Pore Optics Mirror Modules (SPO MMs) [8], which then diffract through the Critical-Angle Transmission (CAT) gratings [9] into a spectrum. The dispersed photons traverse the boom and are detected at the focal plane on one of the two identical Detector Subsystem Assemblies (DSAs). The key components of the spectrometer – the optics, gratings, and detectors – are manufactured using commercial silicon nanofabrication processes, reducing costs and increasing reliability throughout the process. The modular instrument design is verified at multiple subassembly levels. Arcus's 12m focal length and available launch vehicle fairings necessitate a deployable boom with a clear optical path to the detector. *Arcus* uses a high-heritage coilable boom [see, e.g. 19] from Northrop Grumman (formerly OATK/ Goleta) that meets these requirements with modest mass and a high (50:1) compression factor when stowed. A boom prototype has been developed and successfully tested.

Figure 4 [Left] shows a view of *Arcus* directly down the optical axis. The four identical optical channels (Figure 4[Right]) contain two co-aligned petals holding the SPO MMs and the CAT gratings. Each optical petal contains 24 SPO MMs arranged in 6 rows of 4. This is reduced from the 34 SPO MMs in the design used in 2017 *Arcus* proposal, providing a

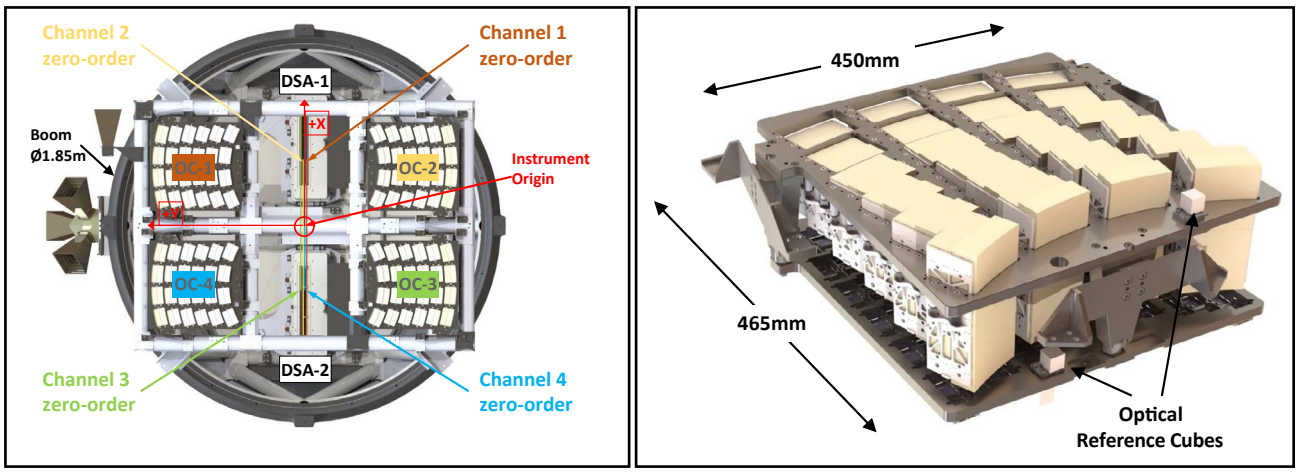

Figure 4: [Left] Schematic of the *Arcus* instrument with four optical channels (OC1-4) each containing multiple MMs and gratings, along with the Detector Subsystem Assemblies. The four channels are identical except to swap the grating blaze to diffract to the left or the right, as appropriate. This modularity reflects *Arcus's* resilience philosophy. The zero order for each channel is on the opposite DSA from the rest of the diffracted spectrum. [Right] An optical channel, showing both the SPO MMs and, on the bottom, the grating petal. The optical reference cubes are used to confirm the petal alignment and the alignment of the channel to the entire system.

significant cost and schedule reduction. This change, however, does not significantly impact throughput due to changes to the SPO MM parameters, specifically using larger pores and a SiC coating [10] that enhances reflectivity.

Arcus' robust design leverages substantial, decades-long investments in NASA's development of high-resolution, efficient lightweight CAT gratings, and ESA's development of SPO MMs. Combining these technologies provides one to two order-of-magnitude improvements (wavelength-dependent) in spectral resolution and collecting area compared with existing X-ray spectrometers. Ths use of *Suzaku*-based CCDs and a *Swift*-based instrument computer, described below, provide flight-proven heritage components.

3.1 Optical Components

The *Arcus* design baselines a a subset of the same SPO MMs being developed for *Athena*, specifically those used in rows #3-8 of the 15 rows planned for *Athena*. SPO MMs use an automated and modular production system that results in high production efficiency at modest expense [11]. In preparation for the *Athena* mission, flight-like SPO MMs successfully underwent performance testing in an X-ray beamline, and environmental testing for vibration, shock, and thermal response [12, 13]. To simplify construction and take maximum advantage of ESA's substantial technology investment, the SPO MMs on *Arcus* are identical to those baselined for *Athena*, including both the same focal length and radii of curvature.

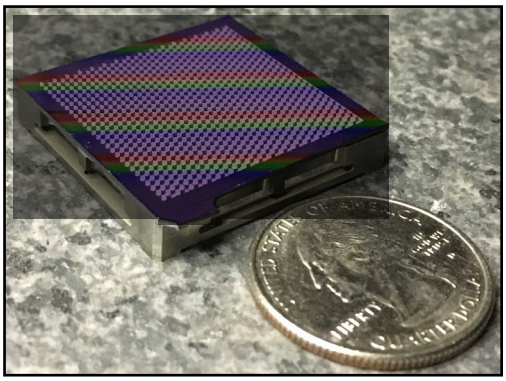

Figure 5: A single CAT grating of the size planned for *Arcus*, mounted on a Ti grating facet.

While a circularly symmetric telescope aperture, such as used by *Athena*, would minimize the boom's cross section, limiting the angular span of the telescope aperture, known as subaperturing [14], allows the design to exploit the anisotropy of the individual SPO MM point spread function. Aligning the spectrometer's dispersion axis to the narrow axis of the telescope PSF results in a narrow line spread function (LSF) and yields high spectral resolving power. The angular extent of this subaperture correlates inversely with the spectral resolving power, so the design limited the azimuthal extent of the OCs to 450 mm across, or < 40°. These constraints lead to a natural division into four identical and independent OCs.

CAT gratings (Figure 5) are blazed transmission gratings that combine the high efficiency and resolution of blazed reflection gratings with the relaxed alignment tolerances and thermal requirements of conventional transmission gratings. substantial effort has been put into CAT grating manufacturing since the 2017 *Arcus* proposal with the effect of reducing cost and improving yield; see [17] for a complete description. The SPO MMs and CAT gratings are aligned via a system successfully demonstrated multiple times [15]. The alignment methods met requirements and that the high-fidelity Arcus ray-trace model reproduces, in detail, the experimental results [16].

Both the optics and gratings technologies have advanced since Phase A [see, e.g. 17,18]. Individual SPO MMs and CAT gratings have been tested at NASA Marshall Space Flight Center's Stray Light Facility [9] and exceeded the Arcus requirements.

3.2 Detectors and Instrument Control Unit

The detector subsystem architecture and its major components have heritage from *Suzaku* and *TESS*. The *Arcus* CCDs are CCID-94 backside illuminated (BI) devices designed and manufactured specifically for *Arcus* by MIT Lincoln Laboratory (MIT/LL). They derive directly from the CCID-41 devices flown on *Suzaku* [20] and the CCID-17 devices flown on *Chandra*, and share many design features of those BI detectors: 24 mm pixel size, 45 mm thickness (fully depleted), frame store design, and charge injection capability. The 2048x1024 pixel CCDs are identical in height to those previous versions, but twice as wide to more effectively cover the focal plane with fewer devices. Each CCD has 8 output nodes to allow short read out times while clocking sufficiently slowly to ensure low readout noise (<4e^-). These characteristics satisfy the *Arcus* requirements to detect X-ray photons with high efficiency and determine their energy, arrival time, and detector position. Each detector has an optical blocking filter which serves to reduce low-energy photons and provide protection against contamination, as well as an directly-deposited Al layer for IR blocking [21]. The CCDs are passively cooled and heater controlled to -90±0.5C like *Chandra*, ensuring adequate spectral resolution for order-separation.

The Instrument Control Unit (ICU) performs all *Arcus* processing and data formatting, and it coordinates all activities on the *Arcus* instrument (with the exceptions of boom deployment, which is triggered by the spacecraft). The ICU is responsible for sending commands to and receiving data from the Forward Data Sending Unit (FDSU) and the the Detector

Electronics, as well as collecting housekeeping (HK) data from the instrument and extracting event data from the CCD images. It formats science and HK data and passes packets to the S/C for transmission to the ground. The ICU is built by Southwest Research Institute (SwRI) and has flight heritage from *MMS* CIDP, *Juno* JADE, and *Swift* XEP.

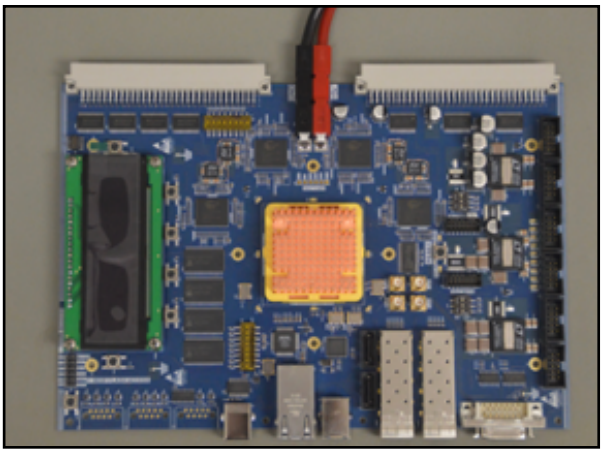

Figure 6: ERP TRL 5 demonstration board

The ICU contains the Digital Board (DB), the Power/Analog Board (PAB), and the Event Recognition Processor (ERP) board. The DB and backplane are near build-to-print copies of the *MMS* CPU system, with only minor changes to interfaces using heritage (TRL 7+) designs. The DB hosts a Leon2FT SPARC processor running at up to 100 MHz, an RTAX2000S FPGA, an external RS-422 UART GSE port, and dual 115 kbps RS-422 UART command/telemetry interfaces to the S/C bus. UARTs are also used to send commands to and receive housekeeping from the detector electronics (RS-422), and FDSU (115 kbps LVDS).

The PAB has heritage from MMS CIDP. It connects to the +28VDC S/C bus and distributes +3.3V digital power and ±5V analog power internally. It contains electronic switches to control unregulated power distribution to the Metrology System, Detector Electronics, and detector doors (redundant). It supports digital I/O, discrete signal monitors, analog HK channels, and it includes FPGA-based interfaces to on-board circuitry and the cPCI interface to the backplane for control and readout by the DB. The PAB is TRL 7+. The ERP reads the CCD images and extracts X-ray events based on acceptable patterns. The processing is done on a Virtex V5 high-speed FPGA (XQR5VFX130), which stores bias images, subtracts bias levels, masks bad pixels, searches for local maxima, and extracts 3×3 event neighborhoods around candidate events. These are sent to the DB for formatting, possible compression, and transmission to the S/C. Prototype ERP development was supported by a NASA SAT grant, and the result of this work was certified as TRL 5 in 2017 by a NASA PCOS review board. The brass board used for this development is shown in Figure 6. Further development to TRL 6 is awaiting funding, with the *Arcus*-specific changes being a straight-forward increase in the overall amount of on-board SRAM (increased to 640 Mbit), the backplane interface conversion to cPCI, and all unnecessary high-speed communications/interface circuitry being removed. Engineering analysis and simulation of this configuration yields >60% margin on all FPGA resources.

Achieving high spectral resolution requires accurate reconstruction of the pointing direction for each detected photon. *Arcus* uses star trackers and an optical metrology system mounted on the front and rear of the instrument to reconstruct motions of a few arcseconds on timescales of seconds to an hour. The position of the instrument's zero-order image, together with thermistors mounted throughout the instrument, track longer-term variation.

4. MISSION

A high-heritage OATK spacecraft (S/C) meets all instrument and mission requirements with robust technical margins. *Arcus* uses the LEOStar-2 S/C bus as its core and the basis for its ADCS, C&DH, Telecom, Power, and Thermal subsystems, allowing substantial reuse of *TESS* and *ICON* GSE. The *Arcus* S/C at launch is <4m high with a diameter <2m and a total mass of <1200 kg, comfortably fitting within the capabilities of the standard launch vehicle services provided for MIDEX missions. The S/C provides continuous power to the instrument, with batteries designed to survive worst-case eclipses. The S/C connection to the Rear Assembly (RA) of the instrument is thermally isolated. This bus is also used by *NuSTAR* with a similar instrument configuration and has been adapted for the *TESS* mission to the High Earth Orbit (HEO) environment. Arcus meets the requirement for high efficiency observing from a stable platform via a 4:1 lunar resonant orbit [22]. The mission design enables continuous operations, and the ~6.8-day period HEO provides a benign radiation environment, low disturbance torques and long-term orbit stability. Science operations are simple, with long, low-jitter, inertially-pointed observations. The simplicity of operations in the HEO environment leads to a high (>84%) observing efficiency ensuring that all science observations can be accomplished within 18 months of the 2-year baseline science phase, providing 6 months of margin. The flight system consumables are sized for 10 years to enable possible extended operations.

NASA/ARC will host the *Arcus* Mission Operations Center (MOC) as part of the ARC Multiple Mission Operations Center (MMOC). The ARC MMOC has successfully managed mission operations for a number of Explorer-class missions such as Kepler, *LCROSS*, *LADEE* and *IRIS*. The Smithsonian Astrophysical Observatory (SAO) provides the Science Operations Center (SOC), working closely with ARC. SAO hosts and operates multiple science operations centers ranging in scale from

Explorer-sized (*Hinode*) to flagship (*Chandra*). The *Arcus* science requirements allow a stable and simple cadence for mission operations. After commissioning, real-time contacts with the S/C via the Deep Space Network are performed once per orbit near perigee to download science data and upload a 2-week long observation schedule. No re-pointing is required for this or the three TT&C contacts that occur at other points in the orbit. Mission operations benefits from a well-defined target list (~350 sources) that can be observed in any order while fully achieving the science objectives. Science data processing reuses software and algorithms developed for *Chandra*, *Suzaku*, and *eRosita*.

5. ACKNOWLEDGMENTS

The *Arcus* Phase A study, upon which much of this work is based, was funded by NASA as part of the 2017 MIDEX call. The *Arcus* team also notes internal funding support from SAO, NASA/ARC, MPE, MIT, PSU, Northrop Grumman, and NASA/GSFC. Special thanks to team members Casey DeRoo, Moritz Günther, Ed Hertz, and Abraham Falcone for input to this presentation.

6. REFERENCES

[1] National Research Council, "New Worlds, New Horizons in Astronomy and Astrophysics" (2010). http://www.nap.edu/catalog/12951/new-worlds-new-horizons-in-astronomy-and-astrophysics.
[2] Kouveliotou, C., et al., "Enduring Quests-Daring Visions (NASA Astrophysics in the Next Three Decades)", ArXiv e-print 1401.3741 (2014). http://ui.adsabs.harvard.edu/abs/2014arXiv1401.3741K.
[3] NASA Science Mission Directorate. "NASA 2014 Science Plan" (2014) https://smd-prod.s3.amazonaws.com/science-green/s3fs-public/atoms/files/2014_Science_Plan_PDF_Update_508_TAGGED.pdf
[4] Rahmati, A., et al., "Cosmic distribution of highly ionized metals and their physical conditions in the EAGLE simulations", Monthly Notices of the Royal Astronomical Society, vol. 459, p. 310 (2016). http://ui.adsabs.harvard.edu/abs/2016MNRAS.459..310R.
[5] Heilmann, R. K., et al., "Critical-angle x-ray transmission grating spectrometer with extended bandpass and resolving power > 10,000", proceedings of the SPIE, vol. 9905, p. 99051X (2016). http://ui.adsabs.harvard.edu/abs/2016SPIE.9905E..1XH.
[6] Tashiro, M. S., et al., "Status of x-ray imaging and spectroscopy mission (XRISM),Proceedings of the SPIE, this vol, Paper 11444-176
[7] Nandra, K., "Athena: Science capabilities and current status of ESA's next generation x-ray observatory", Proceedings of the SPIE, this vol, Paper 11444-23
[8] Collon, M. J., et al., "Development of ATHENA mirror modules", Proceedings of the SPIE Conference Series, vol. 10399, p. 103990C (2017). http://ui.adsabs.harvard.edu/abs/2017SPIE10399E..0CC.
[9] Heilmann, R. K., et al., "Critical-angle transmission grating technology development for high resolving power soft x-ray spectrometers on Arcus and Lynx", proceedings of the SPIE Conference Series, vol. 10399, p. 1039914 (2017). http://ui.adsabs.harvard.edu/abs/2017SPIE10399E..14H.
[10] Massahi, S., et al., "Industrialization of the mirror plate coatings for the ATHENA mission", Proceedings of the SPIE Conference Series, vol. 10399, p. 103991W (2017). http://ui.adsabs.harvard.edu/abs/2017SPIE10399E..1WM
[11] Wille, E., Bavdaz, M., and Collon, M., "Mass production of silicon pore optics for ATHENA", Proceedings of the SPIE, vol. 9905, p. 990529 (2016). http://ui.adsabs.harvard.edu/abs/2016SPIE.9905E..29W
[12] Wille, E., et al., "Qualification of silicon pore optics", Proceedings of the SPIE, vol. 9144, p. 91442H (2014). http://ui.adsabs.harvard.edu/abs/2014SPIE.9144E..2HW.
[13] Landgraf, B., et al., "Environmental testing of the ATHENA mirror modules", Proceedings of the SPIE Conference Series, vol. 10399, p. 103990G (2017). http://ui.adsabs.harvard.edu/abs/2017SPIE10399E..0GL.
[14] Cash, W., "X-ray optics - A technique for high resolution imaging", Applied Optics, vol. 26, p. 2915 (1987). http://ui.adsabs.harvard.edu/abs/1987ApOpt..26.2915C.
[15] Song, J. et al., "Metrology for quality control and alignment of CAT grating spectrometers", Proceedings of the SPIE, Volume 10699, id. 106990S 12 pp. (2018). https://ui.adsabs.harvard.edu/abs/2018SPIE10699E..0SS.
[16] Günther, H. M., Frost, J., and Theriault-Shay, A., "MARXS: A Modular Software to Ray-trace X-Ray Instrumentation", The Astronomical Journal, vol. 154, p. 243 (2017). http://ui.adsabs.harvard.edu/abs/2017AJ....154..243G.
[17] Landgraf, B. et al., "Development and manufacturing of SPO X-ray mirrors", Proceedings of the SPIE, Volume 11119, id. 111190E 8 pp. (2019). https://ui.adsabs.harvard.edu/abs/2019SPIE11119E..0EL
[18] Heilmann, R. et al., "Towards volume manufacturing of high-performance soft x-ray critical-angle transmission gratings", Proceedings of the SPIE Conference Series, this volume.

[19] McEachen, M. E., "Verification of Deployment Precision and Stability Requirements for the GEMS Telescope Optical Boom," in proceeding of the 54th AIAA/ASME/ASCE/AHS/ASC Structures, Structural Dynamics
[20] Koyama, K., et al., "X-Ray Imaging Spectrometer (XIS) on Board Suzaku", PASJ, vol. 59, p. 23 (2007). http://ui.adsabs.harvard.edu/abs/2007PASJ...59S..23K.
[21] Bautz, M., et al., "Directly-deposited blocking filters for high-performance silicon x-ray detectors", Proceedings of the SPIE, vol. 9905, p. 99054C (2016). http://ui.adsabs.harvard.edu/abs/2016SPIE.9905E..4CB.
[22] Plice, L., et al., "Arcus Mission Design: Stable Lunar-resonant High Earth Orbit for X-ray Astronomy," in proceedings of AIAA/AAS Astrodynamics Specialist Conference (2018)
[23] Hernández-Monteagudo, C et al. "Evidence of the Missing Baryons from the Kinematic Sunyaev-Zeldovich Effect in Planck Data", Physical Review Letters, 115, 1301 (2015).
[24] Kovács, O. E., et al., "Detection of the Missing Baryons toward the Sightline of H1821+643", The Astrophysical Journal, 872, 83 (2019).